Neutron average cross sections of ^{237}Np

G. Noguere*
Atomic Energy Commission (CEA), DEN Cadarache, F-13108 Saint Paul Les Durance, France
(Received 8 December 2009; published 16 April 2010)

This work reports ^{237}Np neutron resonance parameters obtained from the simultaneous analysis of time-of-flight data measured at the GELINA, ORELA, KURRI, and LANSCE facilities. A statistical analysis of these resonances relying on average R-matrix and optical model calculations was used to establish consistent l-dependent average resonance parameters involved in the description of the unresolved resonance range of the ^{237}Np neutron cross sections. For neutron orbital angular momentum $l = 0$, we obtained an average radiation width $\langle\Gamma_\gamma\rangle = 39.3 \pm 1.0$ meV, a neutron strength function $10^4 S_0 = 1.02 \pm 0.14$, a mean level spacing $D_0 = 0.60 \pm 0.03$ eV, and a potential scattering length $R' = 9.8 \pm 0.1$ fm.

DOI: 10.1103/PhysRevC.81.044607 PACS number(s): 24.60.Dr, 25.40.Ny, 25.40.Lw, 25.60.Dz

I. INTRODUCTION

Neutron-induced reactions important for transmutation studies have been widely investigated within the frame of a collaboration between the Institute for Reference Materials and Measurements (IRMM) and the French Atomic Energy Commission (CEA). Previous neutron resonance spectroscopy of ^{237}Np, ^{99}Tc, ^{127}I, and ^{129}I are reported in Refs. [1–4]. These works provide consistent sets of s-wave mean level spacing D_0 and neutron strength function S_0. However, statistical analysis of the resolved resonances of the iodine isotopes points out the difficulties in establishing unambiguous average values for higher-order partial waves ($l > 0$).

The focus of the present work is a statistical analysis of the ^{237}Np resonance parameters with methodologies relying on optical model and average R-matrix calculations. The average R-matrix cross sections are parameterized in terms of neutron strength functions S_l and distant level parameters R_l^∞ [5]. At low energy, $R_{l=0}^\infty$ is related to the potential scattering length R'. Optical model calculations were used to establish simple relationships between the s-wave parameters (S_0 and D_0) and the average R-matrix parameters (S_l and R_l^∞).

The R-matrix code CONRAD [6], the optical model code ECIS [7], and the statistical model code TALYS [8] were used to reconstruct ^{237}Np neutron cross sections. Nuclear models implemented in CONRAD are parameterized in terms of neutron strength function S_l, distant level parameter R_l^∞, mean level spacing D_l, and average radiation width $\langle\Gamma_\gamma\rangle$. Comparison of the theoretical cross section with data reported in the literature confirmed the model parameters established in this work.

II. RESONANCE SHAPE ANALYSIS

Neutron resonances of the $n + {}^{237}$Np nuclear system have been studied with data measured at the GELINA facility [1] and with capture cross sections retrieved from EXFOR [9]. Neutron resonances λ were parametrized in terms of resonance energy E_λ, neutron width $\Gamma_{\lambda,n}$, and radiation width $\Gamma_{\lambda,\gamma}$ by using the Reich-Moore approximation of the R-matrix theory [10]. Fission widths were taken from the European library JEFF-3.1 [11].

Measurements carried out at the GELINA facility were performed with the neutron transmission technique. Li-glass detectors (NE912) located 30 and 50 m from the neutron source were used to collect a wide number of experimental data. Detailed descriptions of the experimental setup are given elsewhere [1]. The resolved and unresolved resonance ranges were investigated from 0.3 eV to 2.0 keV by using four NpO_2 samples of different thicknesses. The (n,γ) reaction was analyzed with experimental values measured at the ORELA [12], KURRI [13,14], and LANSCE [15] facilities. The KURRI and LANSCE data sets were used below 10 eV. ORELA data were analyzed up to 100 eV. Tables I and II summarize briefly the main characteristics of the transmission and capture data adopted in our resonance shape analysis.

The least-squares fitting code REFIT [16] was used to adjust the resonance parameters for the data. For transmission data, REFIT simulates the attenuation of the incident neutron beam as follows:

$$T(E) = \int_0^\infty R_E^T(E') \exp\left(-\sum_i n_i \sigma_{t,i}(E')\right) dE', \qquad (1)$$

where i labels the isotopes contained in the sample, n_i stands for the atomic surface density as atoms per barn, $\sigma_{t,i}(E)$ represents the Doppler broadened total cross section, and R_E^T is the experimental resolution of the GELINA spectrometer.

For modeling of the experimental capture cross section, neutron scattering corrections in thin neptunium samples were assumed to be negligible. The following expression of the capture yield was used in our REFIT calculations:

$$Y(E) = N \int_0^\infty R_E^Y(E')\,(1 - T(E'))\frac{\sigma_\gamma(E')}{\sigma_t(E')} dE', \qquad (2)$$

where σ_γ (σ_t) stands for the ^{237}Np Doppler broadened capture (total) cross section, N represents the normalization factor, and R_E^Y is the experimental resolution for the capture measurements.

A preliminary analysis of the low-energy resonances (<10 eV) was reported in Ref. [17]. The latter demonstrates that Monte Carlo techniques can be used to propagate the

*gilles.noguere@cea.fr

TABLE I. Experimental characteristics of the capture data used in this work.

Author(s)	Ref. no.	Facility	Flight length (mm)	Sample diameter (mm)	Sample thickness (at/b)
Weston and Todd	[12]	ORELA	20	50.8	0.25×10^{-3}
Kobayashi *et al.*	[13]	KURRI	12	30	0.35×10^{-3}
Shcherbakov *et al.*	[14]	KURRI	24.2	30	0.35×10^{-3}
Esch *et al.*	[15]	LANSCE	20	6.4	0.0035×10^{-3}

experimental uncertainties during the least-squares fitting procedure. Monte Carlo algorithms and uncertainty propagation techniques are presented in Refs. [18] and [19]. In the present analysis, similar stochastic techniques were used to determine the ^{237}Np resonance parameters up to 500 eV.

Examples of least-squares fits are shown in Fig. 1. Parameters <100 eV are reported in Table III. The given uncertainties take into account the experimental information summarized in Table IV. Comparison of our results with the parameters recommended in the European library JEFF-3.1 points out discrepancies of $<2\%$ on average. However, as shown in Fig. 2, significant discrepancies, $>10\%$, can be observed for the neutron widths. The increasing contribution of the experimental resolution makes unambiguous identification of complex overlapping structures above a few tens of electron volts difficult.

Negative resonances ("external levels") reported in Sec. III were adjusted to accurately reproduce the thermal capture cross section of 180 ± 5 b measured at the ILL facility [20] and the contribution of the shape-elastic cross section observed between the resonances in the transmission data. This analysis yielded a potential scattering length of

$$R' = 9.8 \pm 0.1 \text{ fm}.$$

In the frame of the R-matrix theory, contributions of the direct interaction can be simulated with the so-called distant level parameter R_l^∞. For an s wave, the relationship between R' and R_0^∞ is given by

$$R' = a_c\left(1 - R_0^\infty\right). \tag{3}$$

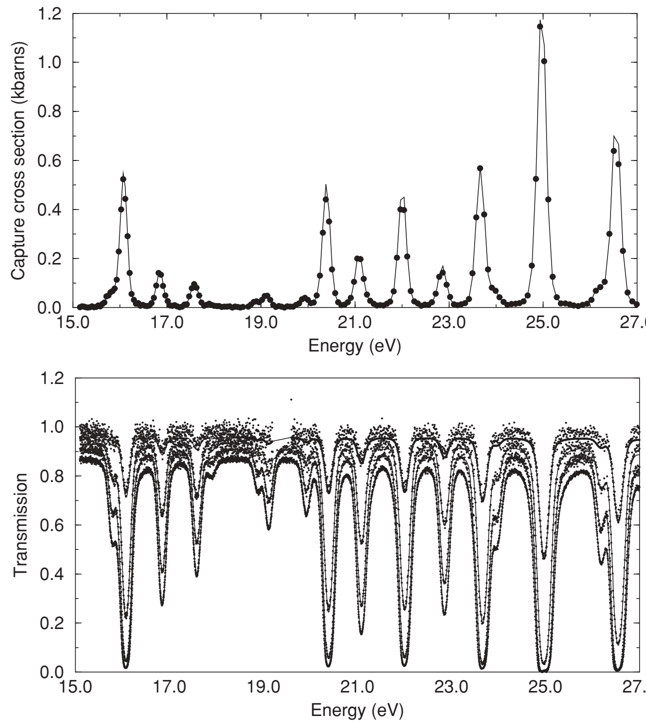

FIG. 1. Examples of $n + {}^{237}$Np resonance peaks observed in the experimental capture cross section measured by Weston and Todd [12] and in the transmission spectra measured by Gressier [1]. Solid lines represent the theoretical curves adjusted by the REFIT code [16].

According to conventions used in the Evaluated Nuclear Data Files [21], the channel radius a_c is defined as follows:

$$a_c = 1.23\left(\frac{A}{m_n}\right)^{1/3} + 0.8 \text{ (fm)}, \tag{4}$$

where $(A/m_n) = 235.012$ is defined as the ratio of the target mass to the neutron mass. By using $a_c = 8.39$ fm and $R' = 9.8$ fm, the s-wave distant level parameter for the $n + {}^{237}$Np nuclear system is

$$R_0^\infty = -0.168 \pm 0.012.$$

The average radiation width was determined from the individual $\Gamma_{\lambda,\gamma}$ values of 19 resonances observed below 23 eV. If they are assumed to be independent, the weighted mean value is close to 39.2 ± 0.2 meV. By taking into account correlation coefficients between the resonance parameters, the mean value

TABLE II. Main characteristics of the transmission measurements performed by Gressier [1] at the GELINA facility.

Date	Flight length (m)	Frequency (Hz)	Sample temperature (K)	"Antioverlap" filter	Sample thickness (at/b)
Feb. 1997	26.453	100	290	Cd	2.49 ± 0.02
Feb. 1997	26.453	100	290	Cd	0.497 ± 0.003
Oct. 1997	49.332	800	300	^{10}B	5.03 ± 0.03
Jan. 1998	26.453	800	300	Cd	7.52 ± 0.04
Feb. 1998	49.332	100	300	Cd	5.03 ± 0.03
June 1998	49.332	800	300	^{10}B	5.03 ± 0.03

TABLE III. ^{237}Np resonance parameters below 100 eV.

E_λ (eV)	J	This work (meV)		JEFF-3.1 (meV)	
		$\Gamma_{\lambda,\gamma}$	$\Gamma_{\lambda,n}$	$\Gamma_{\lambda,\gamma}$	$\Gamma_{\lambda,n}$
-2.8 ± 0.03	2.0	40.0 ± 0.4	2.794 ± 0.050	40.0	2.176
-0.91 ± 0.02	3.0	40.0 ± 0.4	1.182 ± 0.098	40.0	0.450
0.49 ± 0.01	2.0	39.4 ± 0.7	0.047 ± 0.001	40.5	0.047
1.32 ± 0.01	3.0	37.9 ± 0.4	0.031 ± 0.001	40.3	0.032
1.48 ± 0.01	2.0	41.6 ± 0.9	0.184 ± 0.004	40.5	0.184
1.97 ± 0.01	3.0	37.2 ± 0.6	0.014 ± 0.001	39.5	0.014
3.05	[3.0]			40.8	<0.001
3.86 ± 0.01	3.0	40.4 ± 0.6	0.211 ± 0.002	39.7	0.212
4.26 ± 0.01	2.0	40.0 ± 0.9	0.033 ± 0.001	40.4	0.033
4.86 ± 0.01	2.0	40.1 ± 1.2	0.043 ± 0.001	40.0	0.042
5.78 ± 0.01	3.0	42.1 ± 0.8	0.533 ± 0.009	41.9	0.528
6.38 ± 0.01	3.0	38.8 ± 1.2	0.079 ± 0.001	39.6	0.079
6.68 ± 0.01	2.0	39.3	0.014 ± 0.001	40.1	0.013
7.19 ± 0.00	2.0	39.3	0.010 ± 0.001	40.0	0.009
7.42 ± 0.01	3.0	39.0 ± 1.5	0.124 ± 0.001	38.4	0.122
7.67 ± 0.01	2.0	39.3	0.003 ± 0.001	40.0	0.002
8.30 ± 0.01	3.0	39.7 ± 1.4	0.093 ± 0.001	37.6	0.090
8.98 ± 0.01	3.0	37.2 ± 1.3	0.104 ± 0.001	37.0	0.102
9.30 ± 0.01	2.0	41.8 ± 0.9	0.611 ± 0.006	41.4	0.602
10.23 ± 0.01	2.0	39.3	0.030 ± 0.001	40.0	0.028
10.68 ± 0.01	3.0	39.3	0.439 ± 0.005	40.0	0.432
10.84 ± 0.01	3.0	39.3	0.701 ± 0.011	40.0	0.689
11.10 ± 0.01	2.0	42.2 ± 1.1	1.032 ± 0.013	43.8	1.010
12.20 ± 0.01	3.0	39.3	0.048 ± 0.001	40.0	0.049
12.62 ± 0.01	2.0	38.9 ± 1.2	0.925 ± 0.010	40.2	0.911
13.13 ± 0.01	3.0	39.3	0.017 ± 0.001	40.0	0.017
14.39 ± 0.01	2.0	39.3	0.002 ± 0.001	40.0	0.002
15.79 ± 0.01	3.0	39.3	0.069 ± 0.001	40.0	0.069
15.94 ± 0.01	3.0	39.3	0.038 ± 0.001	40.0	0.038
16.08 ± 0.01	2.0	38.1 ± 1.8	1.069 ± 0.012	40.0	1.052
16.86 ± 0.01	2.0	39.3	0.304 ± 0.002	37.8	0.299
17.59 ± 0.01	3.0	39.3	0.159 ± 0.001	39.1	0.156
17.90 ± 0.01	2.0	39.3	0.018 ± 0.001	40.0	0.018
17.94 ± 0.01	3.0	39.3	0.003 ± 0.001	40.0	0.003
18.89 ± 0.02	2.0	39.3	0.048 ± 0.001	40.0	0.048
19.13 ± 0.02	3.0	39.3	0.089 ± 0.001	40.0	0.088
19.92 ± 0.01	3.0	39.3	0.069 ± 0.001	40.0	0.070
20.40 ± 0.01	2.0	37.1 ± 1.9	1.395 ± 0.015	39.4	1.368
21.09 ± 0.02	3.0	39.3	0.450 ± 0.003	40.0	0.446
21.31 ± 0.02	2.0	39.3	0.032 ± 0.001	40.0	0.028
22.01 ± 0.02	2.0	36.5 ± 1.8	1.521 ± 0.018	39.5	1.498
22.86 ± 0.02	3.0	38.2 ± 2.4	0.386 ± 0.003	38.5	0.380
23.67 ± 0.02	3.0	39.3	1.436 ± 0.018	38.0	1.420
23.99 ± 0.02	2.0	39.3	0.182 ± 0.002	40.0	0.191
24.85 ± 0.02	3.0	39.3	0.034 ± 0.006	40.0	0.026
24.98 ± 0.02	3.0	39.3	3.661 ± 0.059	40.0	3.665
26.19 ± 0.02	3.0	39.3	0.196 ± 0.002	40.0	0.199
26.56 ± 0.02	3.0	39.3	2.389 ± 0.039	40.7	2.336
27.09 ± 0.02	2.0	39.3	0.039 ± 0.001	40.0	0.038
28.46 ± 0.02	2.0	39.3	0.093 ± 0.006	40.0	0.094
28.61 ± 0.02	3.0	39.3	0.031 ± 0.007	40.0	0.031
28.93 ± 0.02	2.0	39.3	0.138 ± 0.002	40.0	0.137
29.48 ± 0.02	2.0	39.3	0.083 ± 0.002	40.0	0.084
30.42 ± 0.02	3.0	39.3	3.135 ± 0.055	38.2	3.145
30.74 ± 0.02	2.0	39.3	0.358 ± 0.007	40.0	0.371

TABLE III. *(Continued.)*

E_λ (eV)	J	This work (meV)		JEFF-3.1 (meV)	
		$\Gamma_{\lambda,\gamma}$	$\Gamma_{\lambda,n}$	$\Gamma_{\lambda,\gamma}$	$\Gamma_{\lambda,n}$
31.30 ± 0.02	3.0	39.3	0.245 ± 0.003	40.0	0.245
31.66 ± 0.03	3.0	39.3	0.042 ± 0.001	40.0	0.043
32.48 ± 0.03	2.0	39.3	0.011 ± 0.002	40.0	0.011
33.42 ± 0.02	3.0	39.3	0.395 ± 0.005	40.0	0.395
33.90 ± 0.03	2.0	39.3	0.487 ± 0.006	40.0	0.487
34.08 ± 0.03	3.0	39.3	0.039 ± 0.006	40.0	0.035
34.69 ± 0.03	3.0	39.3	0.163 ± 0.002	40.0	0.170
35.20 ± 0.03	2.0	39.3	0.413 ± 0.004	40.0	0.409
36.38 ± 0.03	3.0	39.3	0.121 ± 0.002	40.0	0.126
36.82 ± 0.03	2.0	39.3	0.085 ± 0.003	40.0	0.087
37.15 ± 0.03	3.0	39.3	1.152 ± 0.011	37.4	1.138
37.83 ± 0.03	2.0	39.3	0.042 ± 0.004	40.0	0.042
38.05 ± 0.03	2.0	39.3	0.208 ± 0.007	40.0	0.208
38.19 ± 0.03	3.0	39.3	1.199 ± 0.013	40.0	1.193
38.91 ± 0.03	3.0	39.3	0.820 ± 0.013	40.0	0.816
39.01 ± 0.03	2.0	39.3	0.410 ± 0.014	40.0	0.410
39.24 ± 0.03	3.0	39.3	0.532 ± 0.007	40.0	0.529
39.80 ± 0.03	2.0	39.3	0.088 ± 0.004	40.0	0.088
39.93 ± 0.03	3.0	39.3	0.453 ± 0.005	40.0	0.450
41.36 ± 0.03	3.0	39.3	1.963 ± 0.027	38.9	1.947
42.38 ± 0.03	3.0	39.3	0.084 ± 0.017	40.0	0.084
42.84 ± 0.03	3.0	39.3	0.083 ± 0.004	40.0	0.083
43.19	3.0			40.6	0.004
43.65 ± 0.03	2.0	39.3	0.345 ± 0.007	40.0	0.339
44.28 ± 0.04	2.0	39.3	0.026 ± 0.012	40.0	0.026
44.92 ± 0.04	2.0	39.3	0.012 ± 0.002	40.0	0.012
45.71 ± 0.04	2.0	39.3	0.516 ± 0.009	40.0	0.511
46.03 ± 0.04	3.0	39.3	0.584 ± 0.010	40.0	0.570
46.36 ± 0.04	3.0	39.3	2.604 ± 0.023	45.3	2.629
47.33 ± 0.04	2.0	39.3	2.900 ± 0.025	38.2	2.863
48.44 ± 0.04	2.0	39.3	0.105 ± 0.006	40.0	0.104
48.77 ± 0.04	3.0	39.3	0.347 ± 0.007	40.0	0.349
48.89 ± 0.04	2.0	39.3	0.172 ± 0.008	40.0	0.172
49.27	2.0			40.0	0.007
49.82 ± 0.04	3.0	39.3	4.194 ± 0.061	36.5	4.169
50.34	2.0			31.3	2.101
50.40 ± 0.04	3.0	39.3	7.399 ± 0.157	46.8	7.396
51.69 ± 0.04	3.0	39.3	0.096 ± 0.005	40.0	0.112
52.21 ± 0.04	2.0	39.3	0.399 ± 0.006	40.0	0.401
52.65 ± 0.04	2.0	39.3	0.886 ± 0.010	40.0	0.880
53.05 ± 0.04	3.0	39.3	0.061 ± 0.005	40.0	0.058
53.89 ± 0.04	2.0	39.3	0.491 ± 0.006	40.0	0.490
54.27 ± 0.04	2.0	39.3	0.167 ± 0.005	40.0	0.157
55.04 ± 0.04	3.0	39.3	0.261 ± 0.004	40.0	0.259
56.02 ± 0.04	2.0	39.3	1.351 ± 0.035	40.0	1.213
56.16 ± 0.05	3.0	39.3	0.613 ± 0.020	40.0	0.718
56.57 ± 0.05	2.0	39.3	0.036 ± 0.007	40.0	0.036
56.86	3.0			40.0	0.013
57.40	2.0			56.0	0.006
58.40 ± 0.04	3.0	39.3	0.397 ± 0.010	40.0	0.372
58.63 ± 0.05	3.0	39.3	0.218 ± 0.007	40.0	0.245
59.51 ± 0.04	2.0	39.3	2.339 ± 0.021	40.0	2.337
60.06 ± 0.04	3.0	39.3	2.325 ± 0.030	40.0	2.274
60.96 ± 0.04	3.0	39.3	1.595 ± 0.018	40.0	1.562
61.37	3.0			40.0	0.015

TABLE III. *(Continued.)*

E_λ (eV)	J	This work (meV)		JEFF-3.1 (meV)	
		$\Gamma_{\lambda,\gamma}$	$\Gamma_{\lambda,n}$	$\Gamma_{\lambda,\gamma}$	$\Gamma_{\lambda,n}$
61.62	3.0			40.2	0.122
61.65 ± 0.04	3.0	39.3	0.451 ± 0.005	40.0	0.452
62.39 ± 0.05	2.0	39.3	0.421 ± 0.035	40.0	0.382
62.50 ± 0.05	3.0	39.3	1.403 ± 0.027	40.0	1.415
62.92 ± 0.05	3.0	39.3	1.529 ± 0.019	40.0	1.485
63.45 ± 0.05	2.0	39.3	0.083 ± 0.005	40.0	0.083
63.95 ± 0.05	3.0	39.3	0.230 ± 0.004	40.0	0.247
64.97 ± 0.05	3.0	39.3	0.867 ± 0.009	40.0	0.855
65.71 ± 0.05	3.0	39.3	4.003 ± 0.069	47.4	3.787
66.36	2.0			40.0	0.028
66.80	2.0			40.8	0.017
67.48 ± 0.05	3.0	39.3	5.070 ± 0.077	42.8	4.866
67.98 ± 0.05	2.0	39.3	2.932 ± 0.034	40.0	2.824
68.78 ± 0.06	3.0	39.3	0.326 ± 0.015	40.0	0.308
69.28	2.0			40.0	0.013
70.26 ± 0.05	3.0	39.3	1.683 ± 0.023	40.0	1.663
70.68 ± 0.06	2.0	39.3	0.598 ± 0.060	40.0	0.624
71.22 ± 0.06	3.0	39.3	2.008 ± 0.200	40.0	1.824
71.48 ± 0.06	2.0	39.3	3.063 ± 0.224	40.0	2.407
71.55	3.0			40.0	0.584
72.30	2.0			40.8	0.005
72.97	2.0			40.0	0.010
73.87 ± 0.06	3.0	39.3	0.278 ± 0.016	40.0	0.276
74.29 ± 0.06	2.0	39.3	1.770 ± 0.044	40.0	1.694
74.59 ± 0.06	3.0	39.3	0.462 ± 0.051	40.0	0.455
75.14 ± 0.06	2.0	39.3	0.170 ± 0.020	40.0	0.146
75.65	3.0			40.0	0.010
76.22 ± 0.06	3.0	39.3	0.029 ± 0.010	40.0	0.029
76.59 ± 0.06	2.0	39.3	0.206 ± 0.017	40.0	0.175
77.00 ± 0.06	3.0	39.3	0.305 ± 0.008	40.0	0.281
77.57 ± 0.06	2.0	39.3	0.033 ± 0.019	40.0	0.033
77.83	3.0			40.8	0.017
78.33 ± 0.06	3.0	39.3	1.383 ± 0.135	40.0	1.470
78.44 ± 0.06	2.0	39.3	0.896 ± 0.200	40.0	0.693
79.28 ± 0.06	2.0	39.3	3.041 ± 0.041	40.0	2.933
79.90	3.0			40.8	0.010
80.39 ± 0.06	2.0	39.3	0.237 ± 0.030	40.0	0.214
80.65 ± 0.06	3.0	39.3	0.460 ± 0.018	40.0	0.428
81.63 ± 0.07	2.0	39.3	0.504 ± 0.015	40.0	0.478
82.13 ± 0.07	3.0	39.3	0.740 ± 0.014	40.0	0.688
82.40	2.0			40.0	0.063
83.43 ± 0.07	2.0	39.3	3.894 ± 0.200	40.0	3.271
83.74 ± 0.06	2.0	39.3	6.526 ± 0.207	40.0	3.152
83.82	2.0			40.0	2.507
85.22 ± 0.07	3.0	39.3	0.935 ± 0.020	40.0	0.933
86.09 ± 0.07	2.0	39.3	0.994 ± 0.060	40.0	1.022
86.53 ± 0.06	3.0	39.3	4.810 ± 0.064	40.0	4.789
87.60 ± 0.06	2.0	39.3	1.950 ± 0.199	40.0	1.626
87.77 ± 0.07	3.0	39.3	1.639 ± 0.150	40.0	1.835
88.18 ± 0.07	3.0	39.3	0.899 ± 0.043	40.0	0.922
88.96 ± 0.07	3.0	39.3	1.561 ± 0.029	40.0	1.602
89.47 ± 0.07	3.0	39.3	3.393 ± 0.058	40.0	3.568
89.94	2.0			40.8	0.068
90.88 ± 0.07	3.0	39.3	4.357 ± 0.064	40.0	4.291
91.01	2.0			40.8	0.362
91.37 ± 0.07	2.0	39.3	0.176 ± 0.036	40.0	0.187
91.99 ± 0.07	3.0	39.3	0.493 ± 0.009	40.0	0.482
92.78 ± 0.07	3.0	39.3	0.178 ± 0.007	40.0	0.160
93.41 ± 0.07	2.0	39.3	2.228 ± 0.031	40.0	2.180
94.25 ± 0.08	3.0	39.3	0.332 ± 0.011	40.0	0.309
94.52 ± 0.08	2.0	39.3	0.100 ± 0.016	40.0	0.098
94.98 ± 0.08	3.0	39.3	0.066 ± 0.006	40.0	0.072
95.43 ± 0.08	2.0	39.3	0.444 ± 0.015	40.0	0.424
96.18 ± 0.08	3.0	39.3	0.071 ± 0.011	40.0	0.076
96.64 ± 0.08	2.0	39.3	0.528 ± 0.016	40.0	0.467
97.39	2.0			40.8	0.018
97.77 ± 0.07	2.0	39.3	4.080 ± 0.054	40.0	3.967
98.51 ± 0.08	2.0	39.3	2.740 ± 0.037	40.0	2.596
99.12 ± 0.08	3.0	39.3	0.080 ± 0.010	40.0	0.098
99.54 ± 0.08	3.0	39.3	1.578 ± 0.040	40.0	1.593
100.23 ± 0.08	3.0	39.3	4.496 ± 0.072	40.0	4.327
101.08 ± 0.08	2.0	39.3	6.437 ± 0.098	40.0	6.218
101.68 ± 0.08	2.0	39.3	1.632 ± 0.128	40.0	1.681
102.02 ± 0.08	2.0	39.3	2.134 ± 0.141	40.0	2.087

and its uncertainty become

$$\langle \Gamma_\gamma \rangle = 39.3 \pm 1.0 \text{ meV}.$$

Table V compares the average radiation width obtained in this work with those reported in the literature. Although our work suggests a slight decrease in $\langle \Gamma_\gamma \rangle$, agreement between the different values remains within the limit of the given uncertainties.

III. STATISTICAL ANALYSIS OF RESONANCE PARAMETERS

The s-wave mean level spacing D_0 and neutron strength function S_0 can be determined from the distribution of the reduced neutron widths. For an s-wave resonance, the reduced neutron width is defined as the ratio of the neutron width to the square root of the resonance energy:

$$\Gamma^0_{\lambda,n} = \frac{\Gamma_{\lambda,n}}{\sqrt{E_\lambda}}. \tag{5}$$

TABLE IV. Experimental uncertainties introduced in the resonance shape analysis.

Parameter	Uncertainty
Normalization capture yield	2.8%
Effective temperature	10 K
Transmission background	0.005–0.01
Transmission flight length	2.0 cm
Initial delay	5.0 ns
Sample composition	0.5%–0.8%

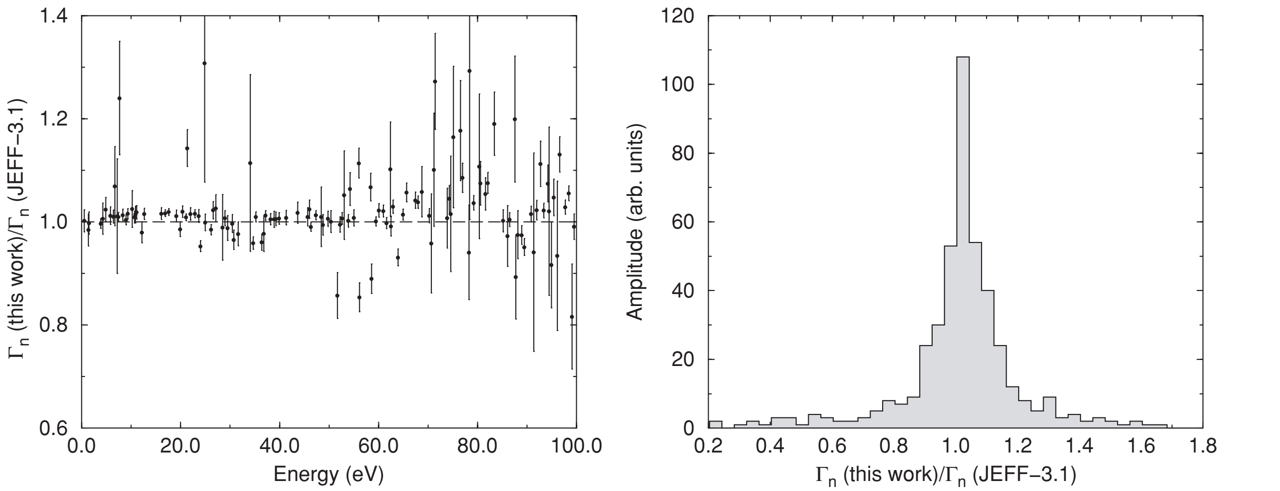

FIG. 2. Comparison of neutron width values obtained in this work and those recommended in the European library JEFF-3.1 below 100 eV. Top: ratio of the neutron widths as a function of the neutron energy. Bottom: distribution of this ratio.

The distribution of this parameter is a chi-square function with 1 degree of freedom [26]:

$$P(x)dx = \frac{e^{-(x/2)}}{\sqrt{2\pi x}}dx, \tag{6}$$

with

$$x = \frac{\Gamma^0_{\lambda,n}}{\langle \Gamma^0_{\lambda,n} \rangle}, \tag{7}$$

where $\langle \Gamma^0_{\lambda,n} \rangle$ stands for the average value of the s-wave reduced neutron width. The relationship among $\langle \Gamma^0_{\lambda,n} \rangle$, D_0, and S_0 can be written as follows:

$$\langle \Gamma^0_{\lambda,n} \rangle = S_0 D_0, \tag{8}$$

with

$$D_0 = \frac{E_{\max} - E_{\min}}{N - 1}, \tag{9}$$

where N stands for the number of s-wave resonances between $E_{\min}$ and $E_{\max}$. This number of resonances can be suggested from the cumulative distribution function of $P(x)$ [Eq. (6)]:

$$N(x_0) = N \int_{x_0}^{\infty} P(x)dx = N\left(1 - \mathrm{erf}\sqrt{\frac{x_0}{2}}\right), \tag{10}$$

TABLE V. ^{237}Np average radiation width obtained in this work and reported in the literature.

Author(s)	Ref. no.	Value (meV)
Paya	[22]	40.0 ± 1.2
Mewissen *et al.*	[23]	41.2 ± 2.9
Weston and Todd	[12]	$\sim$40
Gressier	[1]	40.0 ± 2.0
Noguere *et al.*	[17]	39.5 ± 0.7
Mughaghab	[24]	40.7 ± 0.5
RIPL-2	[25]	40.8 ± 1.2
This work		39.3 ± 1.0

By using expressions (8) and (9), Eq. (10) becomes

$$N(X_0) = \left(\frac{E_{\max} - E_{\min}}{D_0} + 1\right)\left(1 - \mathrm{erf}\sqrt{\frac{X_0}{2S_0 D_0}}\right), \tag{11}$$

with

$$X_0 = x_0 S_0 D_0. \tag{12}$$

This distribution gives the number of resonances λ having a reduced neutron width $\Gamma^0_{\lambda,n}$ higher than a threshold value X_0. This statistical approach is called the ESTIMA method. Detailed explanations are given elsewhere [3].

For the nuclear systems $n + {}^{237}$Np, the only s-wave states of the compound nucleus allowed in the resonance range are those with total angular momenta $J = 2$ and $J = 3$. The corresponding statistical spin factors are $g_{J=2} = 5/12$ and $g_{J=3} = 7/12$. A satisfactory agreement between the theoretical curve [Eq. (11)] and the experimental distribution of the J-dependent reduced neutron widths was observed below $E_{\max} = 90$ eV. Results provided by the ESTIMA method are shown in Fig. 3. The s-wave neutron strength function and mean level spacing can be deduced from the J-dependent values by using the following relationships:

$$S_0 = \sum_{J=2}^{3} g_J S_{0,J}, \tag{13}$$

$$D_0 = \left(\sum_{J=2}^{3} \frac{1}{D_{0,J}}\right)^{-1}. \tag{14}$$

The combination of the J-dependent results provides

$$10^4 S_0 = 1.02 \pm 0.14,$$
$$D_0 = 0.60 \pm 0.03 \text{ eV}.$$

The quoted uncertainties take into account the uncertainties of the resonance parameters (Table III) and of the statistical analysis.

Figure 4 compares the final s-wave results with the "staircase" plots of the reduced neutron widths and of the

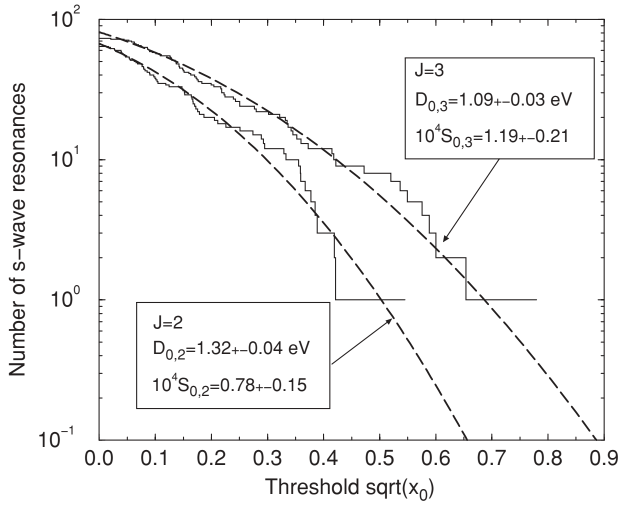

FIG. 3. Cumulative distribution functions of the reduced neutron widths determined in this work (solid lines) and calculated with Eq. (10) (dashed lines). The energy range for the statistical analysis is [$E_{\min} = 0.49$ eV; $E_{\max} = 90$ eV].

cumulated number of resonances. The discrepancies observed on the cumulated number of resonances confirm the increasing number of missing small resonances above 100 eV.

Table VI compares the average parameters obtained in this work with those reported in the literature. Our $10^4 S_0$ and D_0 results are consistent with the expected values close to unity and 0.6 eV, respectively.

IV. *l*-DEPENDENT MEAN LEVEL SPACING

For the nuclear system $n + {}^{237}$Np, the l-dependent mean level spacing D_l can be calculated as follows, assuming equal probability for both parities:

$$\frac{1}{D_0} = \frac{1}{2}\sum_{J=2}^{3} \rho_J(B_n), \tag{15}$$

TABLE VI. ^{237}Np neutron strength function S_0 and mean level spacing D_0 reported in the literature and obtained in this work.

Author(s)	Ref. no.	$E_{\max}$ (eV)	$10^4 S_0$	D_0 (eV)
Slaughter *et al.*	[27]	30	0.96 ± 0.13	1.15 ± 0.12
Mewissen *et al.*	[23]	100	1.02 ± 0.14	0.74 ± 0.06
Weston and Todd	[12]	100	1.02 ± 0.06	0.45 ± 0.10
Gressier	[1]	90	1.00 ± 0.07	0.58 ± 0.03
Mughaghab	[24]		1.02 ± 0.06	0.52 ± 0.04
RIPL-2	[25]		0.97 ± 0.07	0.57 ± 0.03
This work		90	1.02 ± 0.14	0.60 ± 0.03

$$\frac{1}{D_1} = \frac{1}{2}\sum_{J=1}^{4} \rho_J(B_n), \tag{16}$$

$$\frac{1}{D_2} = \frac{1}{2}\sum_{J=0}^{5} \rho_J(B_n). \tag{17}$$

In this work, the J-dependent level density $\rho_J(E)$ was calculated using the formula established by Gilbert and Cameron [28]:

$$\rho_J(E) = \rho(E)\,\frac{2J+1}{4\sigma^2(E)}\exp\left(-\frac{(J+1/2)^2}{2\sigma^2(E)}\right). \tag{18}$$

The parametrization of $\rho(E)$ is given by the constant-temperature approximation ($E < E_m$) and the Fermi-gas model ($E > E_m$),

$$\rho(E) = \begin{cases} \dfrac{1}{T}\exp\left(\dfrac{E-E_0}{T}\right), & E < E_m, \\[2ex] \dfrac{\exp(2\sqrt{a(E-\Delta)})}{12\sqrt{2}a^{1/4}(E-\Delta)^{5/4}\sigma(E)}, & E > E_m, \end{cases} \tag{19}$$

where $\sigma(E)$ stands for the spin cut-off parameter:

$$\sigma^2(E) = 0.0888A^{2/3}\sqrt{a(E-\Delta)}. \tag{20}$$

The pairing energy $\Delta = 0$ because the nuclear system $n + {}^{237}$Np is characterized by odd values of N and Z.

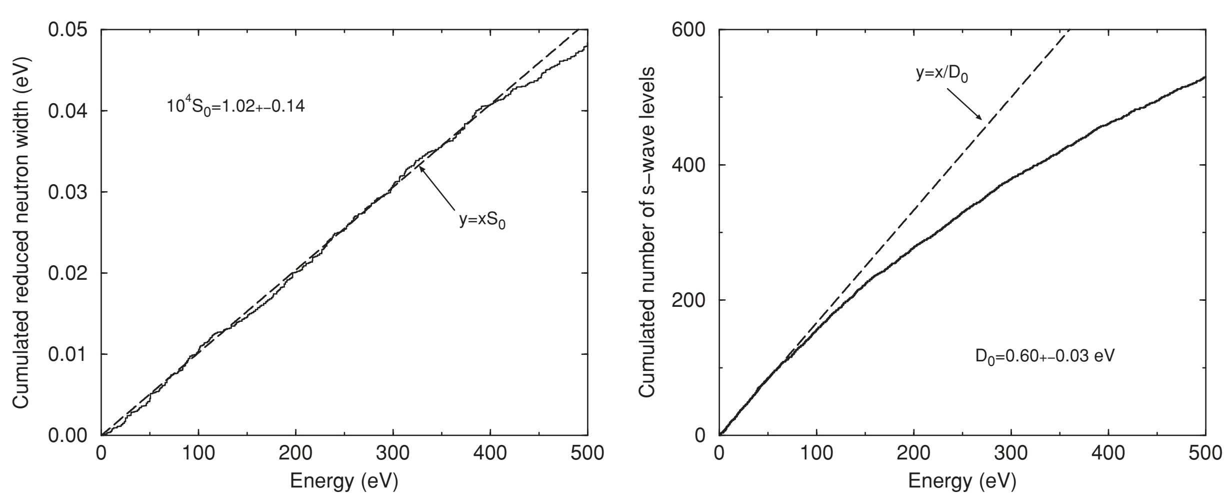

FIG. 4. Comparison of the results provided by the ESTIMA method (dashed line) and "staircase" plots of the s-wave reduced neutron widths (left) and of the cumulative number of s-wave resonances (right).

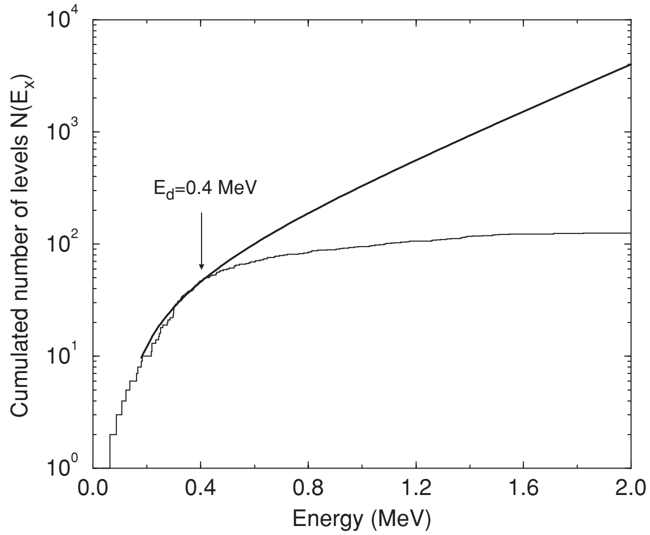

FIG. 5. Cumulated number of levels taken from RIPL [25] for the nuclear system $n + {}^{237}$Np. The solid (lower) curve was calculated with Eq. (21).

The level density parameter a is calculated from the s-wave mean level spacing $D_0 = 0.60 \pm 0.03$ eV. By introducing the Fermi-gas model in Eq. (15), we obtain

$$a = 27.90 \pm 0.12\ \text{MeV}^{-1}.$$

The corresponding mean level spacings for $l = 1$ and $l = 2$ [Eqs. (16) and (17)] are

$$D_1 = 0.309 \pm 0.015\ \text{eV},$$
$$D_2 = 0.218 \pm 0.011\ \text{eV}.$$

The nuclear temperature T was determined by fitting the cumulative numbers of low-lying nuclear levels $N(E_x)$ with the following expressions [29,30]:

$$N(E_x) = N(E_d) + e^{-E_0/T}(e^{E_x/T} - e^{-E_d/T}), \tag{21}$$

$$E_0 = E_m - T \ln\left(\frac{T\exp(2\sqrt{a(E_m - \Delta)})}{12\sqrt{2}a^{1/4}(E_m - \Delta)^{5/4}\sigma(E_m)}\right), \tag{22}$$

$$E_m = \frac{T}{2}(aT - 3 + \sqrt{aT(aT - 6)}) + \Delta. \tag{23}$$

The value of the nuclear temperature depends on the upper energy level E_d, where the "continuum" is supposed to start. The solid (lower) curve in Fig. 5 was obtained for $E_d = 0.4 \pm$ 0.1 MeV. Results for T, E_m, and E_0 are reported in Table VII. The given uncertainties are dominated by the choice of E_d.

TABLE VII. Parameters involved in the constant-temperature model for the nuclear system $n + {}^{237}$Np.

Parameter	Value in this work
T	0.41 ± 0.01 MeV
E_m	3.33 ± 0.15 MeV
E_0	-1.36 ± 0.09 MeV

V. l-DEPENDENT NEUTRON STRENGTH FUNCTION

The l-dependent neutron average parameters of interest in this work are the neutron strength function S_l and the distant level parameter R_l^∞. Within the frame of the average R-matrix theory proposed by Frohner [5], the neutron total cross section is given by

$$\sigma_t(E) = \frac{2\pi}{k^2}\sum_l (1 - \text{Re}[U_l(E)]), \tag{24}$$

in which U_l represents the collision matrix elements,

$$U_l(E) = e^{-2i\varphi_l(E)}\frac{1 + i\,P_l(E)R_l^\infty - s_l P_l(E)\pi}{1 - i\,P_l(E)R_l^\infty + s_l P_l(E)\pi}, \tag{25}$$

where P_l and φ_l are, respectively, the penetration factor of the centrifugal barrier and the phase shift of the incident wave scattered by a sphere. The parameter s_l stands for the pole strength function, which is closely related to the strength function S_l:

$$s_l = \frac{S_l\sqrt{E}}{2ka_c}. \tag{26}$$

Above a few tens of kilo–electron volts, the increasing contribution of the higher-order partial waves makes it impossible to separate the cross sections into l-dependent parameters. This problem was recently solved with the generalized SPRT method [31]. The latter method establishes simple relationships between the optical model and the average R-matrix parameters. According to this method, the energy dependence of the distant level parameter and pole strength function is given by

$$R_l^\infty(E) = \frac{2a_l(E)\cos[2\varphi_l(E)] + (1 - 2b_l(E))\sin[2\varphi_l(E)]}{P_l(E)\big(1 + 2c_l^2(E) - 2b_l(E) + (1 - 2b_l(E))\cos[2\varphi_l(E)] - 2a_l(E)\sin[2\varphi_l(E)]\big)}, \tag{27}$$

$$s_l(E) = \frac{2(b_l(E) - c_l^2(E))}{\pi\,P_l(E)\big(1 + 2c_l^2(E) - 2b_l(E) + (1 - 2b_l(E))\cos[2\varphi_l(E)]\big) - 2a_l\sin[2\varphi_l(E)]}, \tag{28}$$

with

$$a_l^2(E) = c_l^2(E) - b_l^2(E), \tag{29}$$

$$b_l(E) = \frac{1}{2l + 1}\sum_{j=l-1/2}^{l+1/2}\ \sum_{J=|j-5/2|}^{j+5/2} g_J \text{Im}\big[C_{lj}^J(E)\big], \tag{30}$$

TABLE VIII. Optical model parameters, uncertainties, and correlation matrix obtained in this work.

Parameter			Relative uncertainty	Correlation matrix						
r_0	(fm)	1.23 ± 0.02	1.6%	100						
a	(fm)	0.63 ± 0.03	5.3%	−8	100					
V_{HF}	(MeV)	-82.7 ± 4.4	5.3%	98	−8	100				
A_v	(MeV)	-15.2 ± 0.5	3.3%	9	−17	5	100			
A_s	(MeV)	-12.7 ± 0.9	7.1%	9	−6	5	4	100		
β_2		0.207 ± 0.010	4.8%	−37	11	−35	−16	−5	100	
β_4		0.102 ± 0.004	3.9%	−37	−8	−32	9	1	−34	100

$$c_l^2(E) = \frac{1}{2l+1} \sum_{j=l-1/2}^{l+1/2} \sum_{J=|j-5/2|}^{j+5/2} g_J \left|C_{lj}^J(E)\right|^2. \qquad (31)$$

In the present work, the optical model code ECIS [7] was used to calculate the collision matrix elements C_{lj}^J involved in Eqs. (29) to (31). As suggested by the work on neptunium reported in Ref. [32], optical model parameters established by Morillon *et al.* [33,34] are suitable to reproduce the direct contribution in $n + {}^{237}\mathrm{Np}$ reactions up to several tens of mega–electron volts (see Appendix).

Consistent l-dependent average parameters can be deduced from the reduced neutron width values $\Gamma^0_{\lambda,n}$ and the potential scattering R' by introducing Eq. (28) into Eq. (11) and Eq. (27) into Eq. (3). This statistical approach was successfully used to analyze the ^{242}Pu neutron cross sections [35] and the unresolved resonance range of the hafnium isotopes [36].

Realistic uncertainties in the average resonance and optical model parameters were determined by using a Monte Carlo technique specifically designed to derive model parameter uncertainties without changing the value of the parameters [37]. Optical model parameters of interest for the uncertainty propagation analysis are the reduced radius r_0, the diffuseness a, the depths (V_{HF}, A_v, and A_s), and the deformation parameters (β_2 and β_4). A collection of ECIS results (total cross section, neutron transmission coefficient, collision matrix element, neutron strength function, distant level parameter, etc.) was generated by randomly varying these optical model parameters according to uniform distributions. Posterior values were selected according to the potential scattering length ($R' = 9.8 \pm 0.1$ fm) and neutron strength function ($10^4 S_0 = 1.02 \pm 0.14$) obtained in Secs. II and III. Final results, reported in Table VIII, were deduced from the first two moments of the posterior distributions. Figure 6 illustrates the strong correlation (∼0.98) obtained between the reduced radius r_0 and the depth V_{HF}.

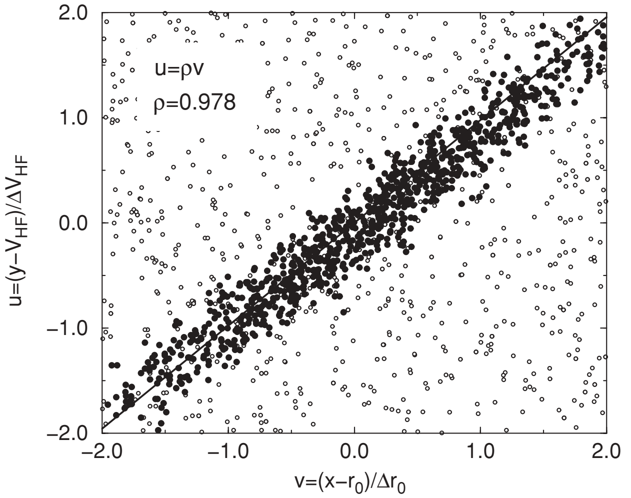

FIG. 6. Correlation between the Hartree-Fock contribution V_{HF} and the reduced radius r_0. Open circles represent the uniform distribution of the prior values. Filled circles represent the posterior values obtained for $10^4 S_0 = 1.02 \pm 0.14$ and $R' = 9.8 \pm 0.1$ fm.

The distributions of the l-dependent average parameters [Eqs. (27) and (28)] are shown in Fig. 7. Table IX reports results for the s-, p-, and d-wave parameters. The s-wave distant level parameter $R_0^\infty = -0.18 \pm 0.03$ gives a potential scattering length $R' = 9.9 \pm 0.25$ fm [see Eq. (3)]. The latter uncertainty is twice as large as the uncertainty determined in the resonance range. By contrast, the final S_0 value of 1.01 ± 0.13 is in excellent agreement with the expected value of 1.02 ± 0.14 reported in Sec. III. Average parameters obtained in this work are summarized in Table X and compared with values compiled in the *Atlas of Neutron Resonances* [24] and RIPL-2 [25].

VI. NEUTRON CROSS SECTIONS

The parametrization established in this work (see Tables VIII and IX) was verified with experimental data retrieved from the EXFOR database [9]. For the total cross section, time-of-flight data measured by Gressier [1], Auchampaugh *et al.* [38], and Paya [22] were averaged over a

TABLE IX. Average R-matrix parameters, uncertainties, and correlation matrix obtained in this work.

Parameter		Relative uncertainty	Correlation matrix					
$10^4 S_0$	1.01 ± 0.13	12.9%	100					
$10^4 S_1$	1.81 ± 0.37	20.4%	19	100				
$10^4 S_2$	1.57 ± 0.23	14.6%	92	24	100			
R_0^∞	-0.18 ± 0.03	16.7%	−19	60	−38	100		
R_1^∞	0.18 ± 0.02	11.1%	−11	65	−15	85	100	
R_2^∞	-0.10 ± 0.03	30.0%	−4	61	−25	98	86	100

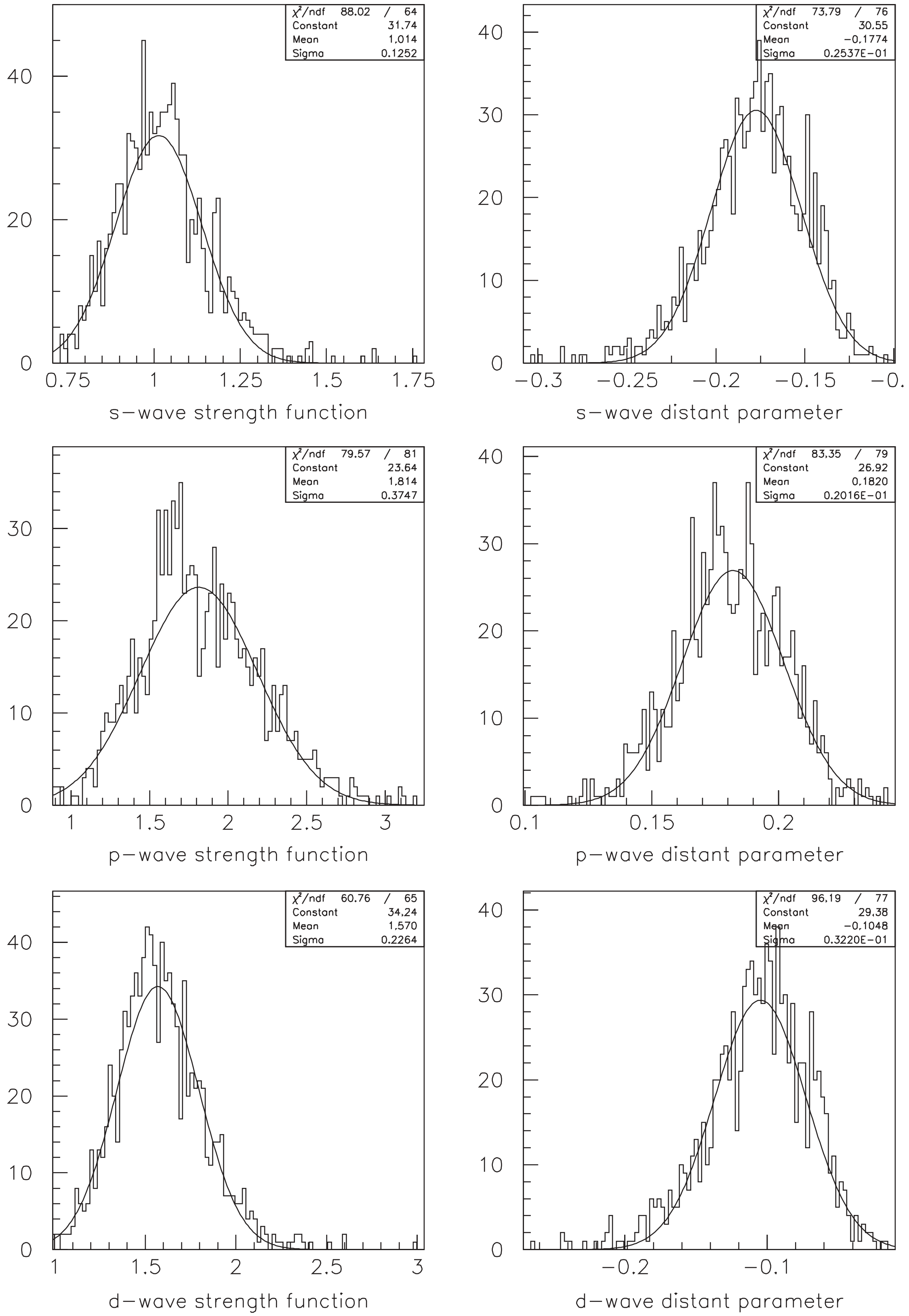

FIG. 7. Posterior distributions of the neutron strength function S_l (left-hand plots) and distant level parameters R_l^{∞} (right-hand plots) for $l = 0, 1, 2$.

TABLE X. Comparison of l-dependent neutron strength functions obtained in this work (ESTIMA and SPRT methods) and reported in the literature.

	ESTIMA	SPRT	Mughaghab [24]	RIPL2 [25]
$10^4 S_0$	1.02 ± 0.14	1.01 ± 0.13	1.02 ± 0.06	0.97 ± 0.07
$10^4 S_1$		1.81 ± 0.37	2.0 ± 0.2	
$10^4 S_2$		1.57 ± 0.23		

suitable energy mesh and corrected for finite-sample-thickness effects. The SESH and CALENDF codes [39,40] were used to calculate this sample thickness correction by generating resonances with Monte Carlo techniques. The SESH code uses the single-level Breit-Wigner formalism to calculate neutron cross sections, while the CALENDF code uses the multilevel Breit-Wigner formalism. The latter is able to account for level-level interferences. This technique is routinely used within the neutron spectroscopy community [41,42] to calculate average total cross sections $\langle \sigma_t(E) \rangle$ from average transmission data $\langle T(E) \rangle$ by combining the sample thickness correction $C_T(E)$ and the sample thickness n (atoms per barn) as follows:

$$\langle \sigma_t(E) \rangle = -\frac{1}{n} \ln \frac{\langle T(E) \rangle}{C_T(E)}. \tag{32}$$

Correction factors $C_T(E)$ obtained for the Paya and Auchampaugh *et al.* data are compared in Fig. 8. A good agreement is obtained between the SESH and the CALENDF codes. The discrepancies remain lower than 5%. They become negligible above 2 keV. Similar calculations were performed for the transmission data measured at the GELINA facility.

The top plot in Fig. 9 compares the experimental data with the total cross section provided by the optical model code ECIS [7]. Calculations performed with and without correlations between the optical model parameters demonstrate the significant impact of our retroactive analysis up to 100 keV.

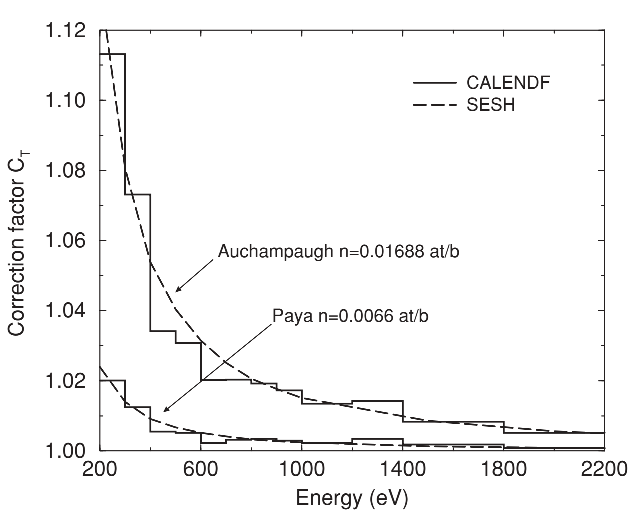

FIG. 8. Sample thickness corrections calculated with the SESH and CALENDF codes for transmission data measured by Paya [22] and Auchampaugh *et al.* [38].

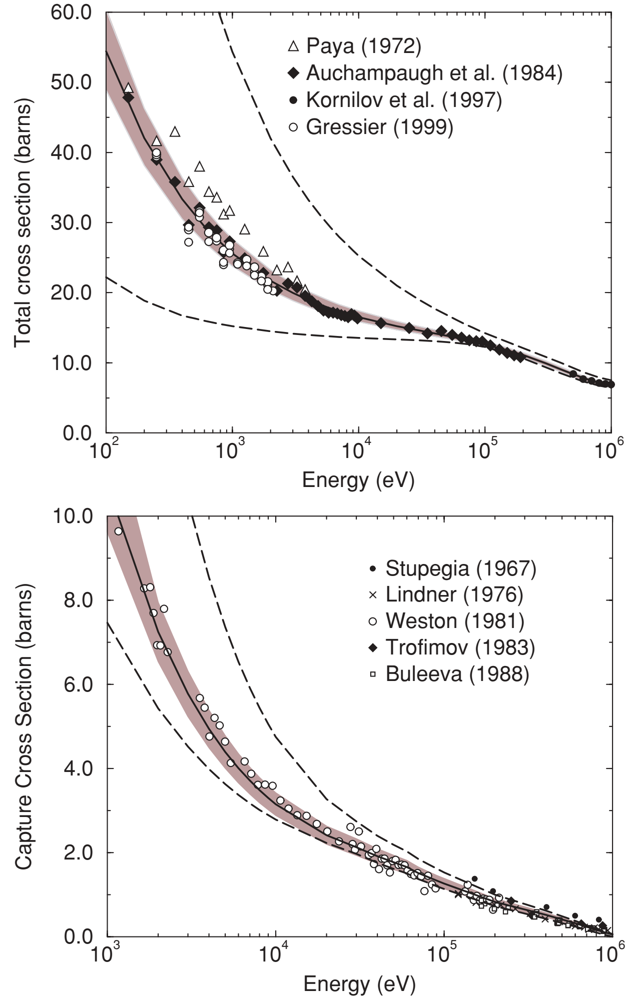

FIG. 9. (Color online) ^{237}Np cross sections (solid line) and uncertainties (shaded area) calculated by ECIS and TALYS. Dashed lines represent the uncertainties calculated without correlations between the model parameters. Experimental data were retrieved from the EXFOR database [9].

The good agreement observed between the data measured by Auchampaugh *et al.* and those measured by Gressier confirms the correct parametrization of the direct interaction used in this work.

The bottom plot in Fig. 9 shows the ^{237}Np capture cross section calculated with the statistical model code TALYS [8]. The correlations among the optical model parameters (Table VIII), the uncertainty of 1.0 meV quoted for the average radiation width (Table V), and the 5% relative uncertainty obtained in the mean level spacing (Table VI) were propagated through the TALYS calculations via direct Monte Carlo techniques [18]. The good agreement obtained with the capture cross section measured at the ORELA facility [12] confirms the magnitude of the ^{237}Np γ-ray strength function $10^4 S_\gamma = 655 \pm 37$ provided by the statistical analysis of the resolved resonance parameters.

The ^{237}Np total and capture cross sections obtained in this work are given in Table XI. Results provided by the ECIS and TALYS codes are compared with those calculated

TABLE XI. ^{237}Np total and capture cross sections (barns) calculated with the ECIS, TALYS, and CONRAD codes below 200 keV.

Energy (keV)	Total cross section		Capture cross section	
	CONRAD	ECIS	CONRAD	TALYS
0.5	31.11	31.23 ± 2.64	16.11	15.90 ± 1.76
0.6	29.47	29.58 ± 2.43	14.54	14.35 ± 1.57
0.8	27.15	27.28 ± 2.13	12.35	12.19 ± 1.30
1.0	25.57	25.71 ± 1.93	10.88	10.74 ± 1.12
2.0	21.67	21.82 ± 1.43	7.33	7.25 ± 0.71
3.0	19.94	20.09 ± 1.22	5.85	5.78 ± 0.54
4.0	18.92	19.07 ± 1.09	5.00	4.94 ± 0.45
5.0	18.21	18.37 ± 1.00	4.44	4.39 ± 0.39
6.0	17.70	17.85 ± 0.93	4.06	4.00 ± 0.35
7.0	17.30	17.45 ± 0.88	3.76	3.71 ± 0.32
8.0	16.97	17.12 ± 0.84	3.53	3.49 ± 0.30
9.0	16.70	16.85 ± 0.80	3.34	3.30 ± 0.28
10.0	16.47	16.62 ± 0.77	3.19	3.15 ± 0.27
20.0	15.19	15.32 ± 0.60	2.45	2.42 ± 0.22
30.0	14.57	14.68 ± 0.52	2.16	2.13 ± 0.20
40.0	14.16	14.24 ± 0.47	1.93	1.91 ± 0.18
50.0	13.83	13.90 ± 0.44	1.79	1.77 ± 0.17
60.0	13.56	13.61 ± 0.41	1.65	1.67 ± 0.15
70.0	13.33	13.35 ± 0.39	1.51	1.52 ± 0.14
80.0	13.11	13.12 ± 0.38	1.41	1.42 ± 0.13
90.0	12.91	12.90 ± 0.37	1.32	1.34 ± 0.12
100.0	12.72	12.70 ± 0.36	1.25	1.27 ± 0.12
200.0	11.20	11.10 ± 0.34	0.79	0.83 ± 0.08

with the CONRAD code [6]. The latter uses the average R-matrix theory [Eqs. (24) and (25)] to calculate the total cross section with the average parameters reported in Table IX. The same code calculates the compound nucleus reactions (capture, elastic, inelastic, and fission reactions) via the Hauser-Feshbach formula with width fluctuation corrections based on the Moldauer's prescriptions. The good agreement between ECIS/CONRAD and TALYS/CONRAD demonstrates the correct description of the cross sections with the l-dependent average parameters established in this work.

VII. CONCLUSIONS

Results presented in this work demonstrate the performance of the combined analysis of the resolved and unresolved resonance ranges to predict the behavior of the neutron-induced capture reaction up to several tens of kilo–electron volts. The good agreement between the theoretical and the experimental values is confirmed by the uncertainties obtained with Monte Carlo techniques.

The analysis of several time-of-flight data provided a potential scattering length $R' = 9.8 \pm 0.1$ fm, an average radiation width $\langle\Gamma_\gamma\rangle = 39.3 \pm 1.0$ meV, an s-wave mean level spacing $D_0 = 0.60 \pm 0.03$ eV, and an s-wave neutron strength function $10^4 S_0 = 1.02 \pm 0.14$. For higher-order partial waves ($l > 0$), the statistical analysis of the resonances with the generalized SPRT method led to p- and d-wave neutron strength functions equal to $10^4 S_1 = 1.81 \pm 0.37$ and $10^4 S_2 = 1.57 \pm 0.23$. By introducing these l-dependent average parameters in the average R-matrix code CONRAD, we obtained total and capture cross sections in excellent agreement with the ECIS and TALYS calculations.

Investigations of the complex nuclear mechanisms involved above the mega–electron volt energy range are in progress. Works performed by A. Tudora at the Faculty of Physics of the University of Bucharest will be used to describe the fission process.

ACKNOWLEDGMENTS

The author wishes to express his appreciation for the work of A. Lepretre, F. Gunsing, A. Brusegan, and P. Siegler. Special thanks go to V. Gressier, who performed the transmission measurement at the GELINA facility. I also express my gratitude to A. Tudora for her relevant advice. The author thanks P. Schillebeeckx and O. Litaize for the correction of this work.

APPENDIX: OPTICAL MODEL POTENTIAL FOR ECIS CALCULATIONS

This Appendix presents the optical model parametrization used to calculate the collision matrix elements C^J_{lj} involved in Eqs. (29) to (31). The dispersive optical potential proposed by Morillon *et al.* [33,34] can be written as

$$\begin{aligned}V(r,E) &= [(V_v(E)+\Delta V_v(E))+iW_v(E)]f(r,r_0,a)\\ &\quad -4a[\Delta V_s(E)+iW_s(E)]\frac{df(r,r_0,a)}{dr}\\ &\quad -[(V_{so}(E)+\Delta V_{so}(E))+iW_{so}(E)]\left(\frac{h}{m_\pi c}\right)^2\\ &\quad \times\frac{1}{r}\frac{df(r,r_0,a)}{dr}\vec{l}\cdot\vec{s},\end{aligned} \tag{A1}$$

where the Woods-Saxon form factors $f(r,r_0,a)$ for the volume (v), surface (s), and spin-orbit (so) potentials share the same geometrical parameters (reduced radius r_0, diffuseness a).

TABLE XII. Optical model parameters established by Morillon *et al.*Values of parameters are reported in Refs [33] and [34].

Parameter	Value
r_0	1.231 fm
a	0.633 fm
V_{HF}	−82.8 MeV
β	1.114 fm
γ	0.093 fm
A_v	−15.24 MeV
B_v	90.44 MeV
A_s	−12.73 MeV
B_s	13.0 MeV
C_s	0.025 MeV

In the dispersion relation treatment, $\Delta V_i(E)$ is used to connect the real $V_i(E)$ and imaginary $W_i(E)$ terms of each component ($i = v, s, \mathrm{so}$). For the spin-orbit contributions, $V_{\mathrm{so}}(E)$ and $W_{\mathrm{so}}(E)$ were taken from Ref. [43]. For the real part of the surface potential the Hartree-Fock contribution of the mean field is given by

$$V_v(E) = V_{\mathrm{HF}} e^{\left(-\frac{\mu\beta^2[E-E_F]}{2\hbar^2}\right)} e^{\left(\frac{4\mu^2\gamma^2[E-E_F]^2}{\hbar^4}\right)}. \tag{A2}$$

This contribution is defined by the depth V_{HF}, the reduced mass of the system μ, and the nonlocality ranges β and γ. For the volume and surface imaginary terms, the energy dependences are symmetric about the Fermi energy E_F:

$$W_v(E) = \frac{A_v(E-E_F)^2}{(E-E_F)^2 + B_v^2}, \tag{A3}$$

$$W_s(E) = \frac{A_s(E-E_F)^2}{(E-E_F)^2 + B_s^2} \exp\left(-C_s(E-E_F)\right). \tag{A4}$$

Optical model parameters established by Morillon *et al.* [33,34] are given in Table XII. Parameters of interest in this work are the reduced radius r_0, the diffuseness a, and the depths V_{HF}, A_v, and A_s. For coupled-channel calculations, deformation parameters β_2 and β_4 were retrieved from the Moller and Nix database [44]:

$$\beta_2 = 0.215 \quad \text{and} \quad \beta_4 = 0.102.$$

[1] V. Gressier, CEA/DSM Saclay Report DAPNIA/SPHN-99-04T (1999).
[2] A. Lepretre, A. Brusegan, N. Herault, G. Noguere, and P. Siegler, CEA/DSM Saclay Report DAPNIA-02-374 (2002).
[3] F. Gunsing, A. Lepretre, C. Mounier, C. Raepsaet, A. Brusegan, and E. Macavero, Phys. Rev. C **61**, 054608 (2000).
[4] G. Noguere, O. Bouland, A. Brusegan, P. Schillebeeckx, P. Siegler, A. Lepretre, N. Herault, and G. Rudolf, Phys. Rev. C **74**, 054602 (2006).
[5] F. H. Frohner, Nucl. Sci. Eng. **103**, 119 (1989).
[6] C. De Saint Jean, B. Habert, O. Litaize, G. Noguere, and C. Suteau, in *Proceedings of the International Conference on Nuclear Data for Science and Technology, Nice, France, 2007*, edited by O. Bersillon *et al.* (EDP Sciences, 2008).
[7] J. Raynal, in *Proceedings of the Specialists' Meeting on the Nucleon Nucleus Optical Model up to 200 MeV, Bruyres-le-Chatel, France, 1996* (Nuclear Energy Agency, Paris, 1997).
[8] A. J. Koning, S. Hilaire, and M. C. Duijvestijn, in *Proceedings of the International Conference on Nuclear Data for Science and Technology, Santa Fe, New Mexico, 2004*, edited by R. C. Haight *et al.* (American Institute of Physics, Melville, NY, 2005).
[9] H. Henriksson, O. Schwerer, D. Rochman, M. V. Mikhaylyukova, and N. Otuka, in *Proceedings of the International Conference on Nuclear Data for Science and Technology, Nice, France, 2007*, edited by O. Bersillon *et al.* (EDP Sciences, 2008).
[10] C. W. Reich and M. S. Moore, Phys. Rev. **111**, 929 (1958).
[11] A. Koning *et al.*, in *Proceedings of the International Conference on Nuclear Data for Science and Technology, Nice, France, 2007*, edited by O. Bersillon *et al.* (EDP Sciences, 2008).
[12] L. W. Weston and J. H. Todd, Nucl. Sci. Eng. **79**, 184 (1981).
[13] K. Kobayashi, S. Lee, S. Yamamoto, H. J. Cho, and Y. Fujita, Nucl. Sci. Tech. **39**, 111 (2002).
[14] O. Shcherbakov, K. Furutaka, S. Nakamura, H. Sakane, K. Kobayachi, S. Yamamoto, J. I. Hori, and H. Harada, Nucl. Sci. Tech. **42**, 135 (2005).
[15] E. I. Esch, R. Reifarth, E. M. Bond, T. A. Bredeweg, A. Couture, S. E. Glover, U. Greife, R. C. Haight, A. M. Hatarik, R. Hatarik, M. Jandel, T. Kawano, A. Mertz, J. M. O'Donnell, R. S. Rundberg, J. M. Schwantes, J. L. Ullmann, D. J. Vieira, J. B. Wilhelmy, and J. M. Wouters, Phys. Rev. C **77**, 034309 (2008).
[16] M. C. Moxon and J. B. Brisland, REFIT computer code. Harwell Laboratory Report No. CBNM/ST/90-131/1 (1990).
[17] G. Noguere, D. Bernard, C. De Saint Jean, B. Iooss, F. Gunsing, K. Kobayashi, S. F. Mughabghab, and P. Siegler, Nucl. Sci. Eng. **160**, 108 (2008).
[18] G. Noguere and J.-Ch. Sublet, Ann. Nucl. Eng. **35**, 2259 (2008).
[19] C. De Saint Jean, G. Noguere, B. Habert, and B. Iooss, Nucl. Sci. Eng. **161**, 363 (2009).
[20] O. Bringer, I. Al Mahamid, S. Chabod, F. Chartier, E. Dupont, A. Letourneau, P. Mutti, L. Oriol, S. Panebianco, and C. Veyssire, in *Proceedings of the International Conference on Nuclear Data for Science and Technology, Nice, France, 2007*, edited by O. Bersillon *et al.* (EDP Sciences, 2008).
[21] M. Herman, ENDF-102 Data Formats and Procedures for the Evaluated Nuclear Data File ENDF-6, Brookhaven National Laboratory Report BNL-NCS-44945-05-Rev (2005).
[22] D. Paya, Ph.D. thesis, Université de Orsay, France, 1972.
[23] L. Mewissen, F. Poortmans, E. Cornelis, G. Vanpraet, A. Angeletti, G. Rohr, and H. Weigmann, Nucl. Sci. Eng. **70**, 155 (1979).
[24] S. F. Mughabghab, *Atlas of Neutron Resonances*, 5th ed. (Elsevier, Amsterdam, 2006).
[25] T. Belgya *et al.*, IAEA Nuclear Data Services Report IAEA-TECDOC-1506 (2005).
[26] C. E. Porter and R. G. Thomas, Phys. Rev. **104**, 483 (1956).
[27] G. G. Slaughter, J. A. Harvey, and R. C. Block, Bull. Am. Phys. Soc. **6**, 70 (1961).
[28] A. Gilbert and A. G. W. Cameron, Can. J. Phys. **43**, 1446 (1965).
[29] G. Vladuca, A. Tudora, F.-J. Hambsch, S. Oberstedt, and I. Ruskov, Nucl. Phys. A **720**, 274 (2003).
[30] G. Vladuca, F.-J. Hambsch, A. Tudora, S. Oberstedt, A. Oberstedt, F. Tovesson, and D. Filipescu, Nucl. Phys. A **740**, 3 (2004).
[31] E. Rich, G. Noguere, C. De Saint Jean, and A. Tudora, Nucl. Sci. Eng. **162**, 76 (2009).
[32] G. Vladuca, A. Tudora, B. Morillon, and D. Filipescu, Nucl. Phys. A **767**, 112 (2006).
[33] B. Morillon and P. Romain, Phys. Rev. C **70**, 014601 (2004).
[34] B. Morillon and P. Romain, Phys. Rev. C **74**, 014601 (2006).
[35] E. Rich, A. Tudora, G. Noguere, J. Tommasi, and J.-F. Lebrat, Nucl. Sci. Eng. **162**, 178 (2009).

[36] G. Noguere, E. Rich, C. De Saint Jean, O. Litaize, P. Siegler, and V. Avrigeanu, Nucl. Phys. A **831**, 106 (2009).
[37] B. Habert, C. De Saint Jean, G. Noguere, L. Leal, and Y. Rugama (accepted for publication in Nucl. Sci. Eng.).
[38] G. F. Auchampaugh, M. S. Moore, J. D. Moses, R. O. Nelson, R. C. Extermann, C. E. Olsen, N. W. Hill, and J. A. Harvey, Phys. Rev. C **29**, 174 (1984).
[39] F. H. Froehner, SESH computer code. General Atomic Report GA-8380 (1968).
[40] J-C.H. Sublet, P. Ribon, and M. Coste-Delclaux, User manual for CEA/DEN Cadarache Report CEA-R-6131 (2006).
[41] H. Derrien, L. C. Leal, and N. M. Larson, in Proceedings of PHYSOR-2006 Topical Meeting on Reactor Physics, Vancouver, Canada (2006).
[42] S. Marrone *et al.*, Phys. Rev. C **73**, 034604 (2006).
[43] A. J. Koning and J. P. Delaroche, Nucl. Phys. A **713**, 231 (2003).
[44] P. Moller, J. R. Nix, and W. J. Swiatecki, At. Data Nucl. Data Tables **59**, 185 (1995).